Journal of Drug Delivery Science and Technology 114 (2025) 107389

Contents lists available at ScienceDirect

Journal of Drug Delivery Science and Technology

journal homepage: www.elsevier.com/locate/jddst

Functionalised gold nanoparticles using abietane diterpenoids from *Plectranthus grandidentatus* Gürke for cancer therapy

Gabrielle Bangay [a,b,1], Vera M.S. Isca [a,1], João Morais [c], Jennifer Fernández Alarcón [d], Ana S. Viana [e], Catarina P. Reis [f], Catarina Pereira-Leite [a,g], Ana M. Díaz-Lanza [b], Lucília Saraiva [c], Cristina Fornaguera [d,**], Patricia Rijo [a,f,*]

[a] CBIOS – Universidade Lusófona's Research Center for Biosciences & Health Technologies, Lisbon, Portugal
[b] Universidad de Alcalá de Henares. Facultad de Farmacia, Departamento de Ciencias Biomédicas (Área de Farmacología; Nuevos agentes antitumorales, Acción tóxica sobre células leucémicas, Ctra. Madrid-Barcelona km. 33, Alcalá de Henares, Madrid, 600 28805, Spain
[c] LAQV/REQUIMTE, Laboratório de Microbiologia, Departamento de Ciências Biológicas, Faculdade de Farmácia, Universidade do Porto, Portugal
[d] Grup d'Enginyeria de Materials (GEMAT), Institut Químic de Sarrià (IQS), Universitat Ramon Llull (URL), 08017, Barcelona, Spain
[e] Centro de Química Estrutural, Faculdade de Ciências da Universidade de Lisboa, Portugal
[f] Research Institute for Medicines (iMED.Ulisboa), Faculdade de Farmácia, Universidade de Lisboa, Portugal
[g] LAQV, REQUIMTE, Departamento de Ciências Químicas, Faculdade de Farmácia, Universidade do Porto, Portugal

ARTICLE INFO

Keywords:
Gold nanoparticles
Plectranthus grandidentatus
diterpene
Cytotoxic
Breast cancer

ABSTRACT

Nanoparticles (NPs) are very small particles with distinct properties stemming from their nanometric size and large surface area, setting them apart from bulk materials. NPs provide many benefits, such as high drug loading capacity, specific targeting, prolonged circulation, and minimized side effects. Over the past few years, metal-based NPs, such as gold NPs (AuNPs), have gained special attention due their surface plasmon resonance properties and use in drug and gene delivery, particularly in cancer treatment and theragnostics. Abietane diterpenoids, such as 7α-acetoxy-6β-hydroxyroyleanone (Roy) isolated from *Plectranthus* spp., are known to be cytotoxic agents, ideal for chemotherapeutic applications. Yet, their poor water solubility and low bioavailability limit their therapeutic efficacy. Harnessing the effectiveness of AuNPs, several nanosystems were made using Roy, the natural diterpene, and an ester derivative. After characterization of size, PDI, zeta potential and encapsulation efficiency, antitumour analysis using *in vitro* cancer cell models of breast cancer (MDA-MB-231, 4T1 and MCF7) were used to probe cytotoxic effect. Roy-functionalised AuNPs showed increased antitumour activity when compared with Roy alone, showcasing the improved antitumoral effect of the nanoformulation. In addition, the Roy-functionalised AuNPs showed selectivity for cancer cells over healthy human fibroblast (HDF) cells, a promising incentive for further development of natural diterpenoid nanosystems in cancer therapy.

1. Introduction

Nanoparticles (NPs) exhibit unique properties due to their small size and high surface area-to-volume ratio, which distinguishes them from bulk materials [1]. NPs can be composed of metals, lipids, proteins, polymers, ceramics and organic compounds [2–7]. In fact, a wide range of NPs have been found to exhibit characteristics that are useful in therapeutics [8]. Common advantages of drug-conjugated and functionalised NPs include their large loading capacity for one or more therapeutics, high water solubility, effective and selective release of therapeutics at the target site, extended circulation half-life and reduced incidence of side effects [9–11]. These advantages have accelerated the use of metal nanoparticles in targeted cancer therapy and diagnostics. However, despite the growing interest in functionalised nanoparticles, challenges remain in optimizing drug loading, targeting specificity and overcoming biological barriers. As such, novel hybrid systems that integrate bioactive molecules with metallic nanoparticles show promise in addressing these limitations [12,13].

Metal-based NPs exhibit distinctive characteristics, prompting their common use as carriers of biomolecules, genes and drugs for therapeutics, including cancer [3,14–17]. Gold NPs (AuNPs) are highly

* Corresponding author. CBIOS – Universidade Lusófona's Research Center for Biosciences & Health Technologies, Lisbon, Portugal.
** Corresponding author.
E-mail addresses: cristina.fornaguera@iqs.url.edu (C. Fornaguera), patricia.rijo@ulusofona.pt (P. Rijo).
[1] Shared 1st authorship.

https://doi.org/10.1016/j.jddst.2025.107389
Received 11 March 2025; Received in revised form 31 July 2025; Accepted 8 August 2025
Available online 9 August 2025
1773-2247/© 2025 The Authors. Published by Elsevier B.V. This is an open access article under the CC BY license (http://creativecommons.org/licenses/by/4.0/).

Abbreviations

NPs	nanoparticles
AuNPs	gold nanoparticles
spp.	species
Roy	7α-acetoxy-6β-hydroxyroyleanone
DLS	dynamic light scattering
AFM	atomic force microscopy
PDI	polydispersity index
ZP	Zeta Potential
NTA	nanoparticle tracking analysis
DMEM	Dulbecco's Modified Eagle Medium
FBS	foetal bovine serum
HDF	human dermal fibroblast
DOX	doxorubicin
EPR	enhanced permeability and retention
SRB	sulforhodamine B

notable among metal NPs due to their varying characteristics, which depend on size, shape and surface plasmon properties. Additionally, extensive research highlights the crucial role of AuNPs in drug targeting. For example, spherical AuNPs with a size around 50 nm have demonstrated a higher internalization compared to other NP size [1]. The functionalization of AuNPs also plays an important role; due to their high surface area-to-volume ratio, it is possible to functionalize AuNPs with any type of molecule, such as peptides, glycans, nucleic acids or natural molecules. Lately, the use of natural compounds extracted from plants provide a rich arsenal of molecules with high redox potential, suitable for functionalization, such as flavanones, flavones, fatty acids, amino acids or diterpenoids.

Cytotoxic abietane diterpenoids isolated from *Plectranthus* species (spp.) are known for their antitumoral activity and are targeted for therapeutic applications, particularly in cancer [18–23]. However, these natural diterpenes are extremely hydrophobic, leading to poor aqueous solubility, low membrane penetration and reduced bioavailability when used as drugs [24–26], hindering their overall therapeutic effectiveness [27].

While there are numerous examples in the literature of NPs loaded with pharmacologically active natural products [4,28–30], to the best of our knowledge, there have been few reports of NPs functionalised with bioactive abietane diterpenoids from *Plectranthus* spp. Recently, Ntungwe et al. (2021) [31] reported the attempt to conjugate the royleanone diterpene, 7α-acetoxy-6β-hydroxyroyleanone (Roy, **1**), with squalene, oleic acid and 1-bromododecane self-assembly inducers, in which self-assembly Roy-oleic acid conjugate was successfully synthesized and characterized [31]. Garcia et al. (2018) [22] reported the formation of hybrid NPs, using AuNPs and another very low water-soluble royleanone diterpene, 6,7-dehydroroyleanone, isolated form *Plectranthus* spp., where the prepared nanosystem exhibited improved cytotoxic activity on resistant lung cancer cell lines compared to 6,7-dehydroroyleanone alone [22]. Furthermore, 6,7-dehydroroyleanone was also conjugated with squalene to afford self-assembly DeRoy-squalene NPs [32,33]. Another compound isolated from *Plectranthus* spp., parvifloron D, was used to prepare hybrid NPs with biopolymers and functionalised with α-melanocyte stimulating hormone, to obtain an anti-melanoma selective-delivery drug formulation [34]. In two other studies, parvifloron D was conjugated with albumin to afford NPs that improved selectivity and stability [23,35]. Finally, sustainable and non-toxic ion oxide NPs have been reported using *Plectranthus amboinicus* extract, which showed promising anticancer efficacy, particularly through apoptosis induction [36].

Despite these promising developments, there remains a significant gap in the targeted application of AuNPs functionalised with natural diterpenes from *Plectranthus* spp. for cancer therapy. Most studies to date focus on encapsulation or conjugation rather than direct functionalization via gold-thiol or hydroxyl interactions. This limits insight into structure–activity relationships and surface chemistry effects on drug release and efficacy. Addressing this gap is critical, as functionalizing AuNPs with hydroxyl-rich diterpenoids may offer superior stability, loading efficiency and selective cytotoxicity [37].

The research herein is a continuation of our lab's already promising findings on potential nanoformulations of abietane compounds from *Plectranthus* spp. for cancer therapeutics, as previously described [20–23,31,35,38,39]. More specifically, given the anti-tumour potential of Roy, the following research investigates the potential of AuNPs conjugated with Roy and assesses their antitumour effect in cancer cell lines.

The primary objectives of this study are to: (i) synthesize and characterize Roy-functionalised AuNPs using the citrate reduction method, (ii) evaluate their physicochemical properties, including particle size, morphology, and conjugation efficiency and (iii) assess the cytotoxic activity of these nanosystems against breast cancer cell lines and healthy fibroblasts. By comparing the functionalization efficiency and biological performance of Roy and its ester derivative, this work explores how structural modifications influence nano-bio interactions. Ultimately, the study contributes to the advancement of functionalised natural product-based nanoplatforms for cancer therapy.

2. Materials and methods

2.1. Plant material

The plant *Plectranthus grandidentatus* Gürke was cultivated at the Parque Botânico da Tapada da Ajuda (Instituto Superior Agrário, Lisbon, Portugal) from cuttings sourced from the Kirstenbosch National Botanical Garden (Cape Town, South Africa). Voucher specimens were deposited at the Herbarium João de Carvalho e Vasconcellos (ISA) under the number 841/2007. The plant material used in this study was collected between 2007 and 2008, and consequently dried, stored at room temperature and shielded from light and humidity.

2.2. Extraction and isolation of natural compound, 1

The acetone ultrasonic-assisted extraction method was adapted from Bernardes et al. (2018) [39]. Aerial parts of *P. grandidentatus* were extracted with acetone (LabChem, Pure grade) at room temperature using ultrasound (3 cycles of 30 min at 35 Hz, with a maximum input power of 320 W). The solvent was then evaporated under vacuum at 40 °C. The resulting crude extract was subjected to sequential chromatography (using a mixture of eluents Hexane (Hex, LabChem, commercial grade) and Ethyl Acetate (EtAcO, LabChem, commercial grade): Hex/EtAcO 90:10, 80:20 or 70:30) to purify compound **1** for semi-synthesis. The natural product **1** was isolated as yellow crystal plates, with spectral data consistent with the literature [39,40]. All commercially available reagents were distilled before use.

2.3. Preparation of ester derivative, 7α-acetoxy-6β-hydroxy-12-O-(3-phenyl)propionylroyleanone, 2

The esterification reaction of **1** to **2** was carried out according to the optimized conditions reported by Isca et al. (2024) [41] with the synthesis recently fully described [42]. Briefly, 20 μmol of **1** (1 eq, limiting reagent) was solubilised in pyridine (Merk, 99 %) (0.5 mL) in a 5 mL round bottom flask, with stirring (400 rpm) at room temperature under nitrogen gas. An excess of phenyl-propionyl chloride (Alfaesor, 98 %) was added to the reaction flask and the reaction was followed by thin layer chromatography (eluent dichloromethane (CH_2Cl_2, LabChem, Pure grade) CH_2Cl_2:AcOEt, 97:3) until total consumption of **1**. After the reaction had finished, the solution was concentrated under reduced pressure and the products purified using preparative chromatography.

2.4. Preparation of royleanone-functionalised AuNPs using citrate reduction method

AuNPs were synthesized using a gold precursor (Gold(III) chloride trihydrate, Santa Cruz Biotechnology, 49.1 % of gold), sodium citrate dihydrate (Thermo scientific, 99 %) and Milli-Q water, kept under constant stirring and heat. To begin with, 48 mL of Milli-Q water and 10 mg of sodium citrate were dissolved in 1 mL of Milli-Q water, and the solution was added to a freshly cleaned (using aqua regia) Erlenmeyer. The solution was kept under constant vigorous stirring (900 rpm) and heat until the solution reached boiling point. Next, 2.5 mg of $HAuCl_4$ dissolved in 1 mL of Milli-Q water was added to the solution, maintaining the stirring and heat. The solution was left for 10 min, after which the heating was stopped, and the solution was left to cool down until it reached room temperature (the stirring was maintained during the entire process). Roy (**1** 2.1 mg) was solubilised in 1 mL acetone (5 mM), which was subsequently diluted to a final concertation of 0.1 mM. To 1 mL of solution of **1**, 0.4 mL of the gold NP citrate solution was added, along with 0.6 mL of Milli-Q water (1:1 vol ratio). Finally, the mixture was protected from light and stirred at 800 rpm for 24 h to produce royleanone-functionalised gold citrate NPs (**1_AuCitNPs**).

2.5. Diameter and polydispersity index (PDI) determination of nanoformulations

The mean size and polydispersity index (PDI) of the nanostructures were assessed using dynamic light scattering (DLS) with a ZetaSizer NanoZS (Malvern Co. Ltd., UK), equipped with a He–Ne red light laser ($\lambda = 633$ nm). Measurements were carried out on undiluted samples (70 μL) at a scattering angle of 180° and a constant temperature of 25 °C. Each size measurement was based on 30 runs to ensure greater accuracy, with data analysed using cumulant analysis.

2.6. Morphological characterization of the royleanone AuNPs using atomic force microscopy (AFM)

Particle morphology for royleanone-functionalised AuNPs (**1_AuNPs** and **2_AuNPs**) was analysed using atomic force microscopy (AFM). Briefly, 40 μL droplets of **1_AuNPs** and **2_AuNPs** aqueous suspensions were placed on freshly cleaved mica surfaces and allowed to adhere. The samples were then air-dried overnight at room temperature. Imaging was conducted using peak force tapping and ScanAsyst mode, with a scan rate of 1 Hz on a Multimode 8 HR microscope equipped with a Nanoscope V Controller (Bruker, Coventry, UK). A ScanAsyst-air 0.4 N/m tip model (Bruker, Coventry, UK) was used for imaging and the resulting images were processed with NanoScope V 1.8 software.

2.7. Determination of size using nanoparticle tracking analysis (NTA)

The hydrodynamic diameter and concentration of **AuCitNPs** and **1_AuCitNPs**, (in particles/mL) were measured using nanoparticle tracking analysis (NTA) with a NanoSight NS300 (Malvern Instruments, Amesbury, UK). The instrument featured a blue laser with a wavelength of 488 nm. For sample preparation, the nanoparticles were diluted 1:1 with Milli-Q water to a final volume of 1 mL, targeting a particle concentration between 10^6 and 10^9 particles/mL. Each 1 mL sample was introduced into the sample chamber using a disposable syringe (BD Discardit II, New Jersey, USA). Measurements were taken in triplicate at 22 °C for 1 min. All data were recorded and analysed using the NanoSight NS300 software.

2.8. Conjugation efficiency

After conjugation, the **1_AuNPs** and **2_AuNPs** nanosystems were recovered via centrifugation (Hermle Z323 K centrifuge, Hermle LaborTechnik, Wehingen, Germany) at 20,000 rpm and 15 °C for 10 min. Drug conjugation efficiency (%) was determined by measuring the amount of unbound drug in the supernatant following centrifugation. Quantification was performed using an Agilent Technologies 1200 Infinity Series system with a diode array detector (DAD; Agilent, Santa Clara, CA, USA), equipped with an Eclipse XDB-C18 column (250 × 4.0 mm i.d., 5 μm) from Merck and ChemStation Software (Hewlett-Packard, Palo Alto, CA, USA). Each sample was analysed with a 20 μL injection using a gradient elution composed of solution A (methanol), solution B (acetonitrile), and solution C (0.3 % trifluoroacetic acid in water) as follows: 0 min, 15 % A, 5 % B, 80 % C; 2 min, 70 % A, 30 % B, 0 % C; 10 min, 70 % A, 30 % B, 0 % C; and 15 min, 15 % A, 5 % B, 80 % C. The flow rate was maintained at 1 mL/min, and the column was kept at 29 °C. The total analysis time was 15 min, including column stabilization. Calibration curves (see supplementary materials) with validated parameters were prepared for each compound. All samples were filtered prior to HPLC analysis. For calibration, stock solutions of compound **1** and compound **2** in methanol were prepared and diluted to five and four known concentrations, respectively. The corresponding areas were determined by HPLC analyses. All analyses were carried out in triplicate. All solvents employed in HPLC analyses were from HPLC grade and purchased from Sigma-Aldrich.

2.9. Cell culture

Dulbecco's Modified Eagle Medium (DMEM), foetal bovine serum (FBS), L-glutamine, penicillin G and streptomycin were purchased from Gibco. Human dermal fibroblast (HDF), 4T1 cells and MCF7 cells were cultured in DMEM supplemented with 10 % FBS, 1 % L-glutamine (2 mM) and 1 % antibiotics (100 units penicillin G and 100 μg/mL streptomycin). Cells were maintained in 5 % CO_2 at 37 °C. Fibroblasts were used up to passage 8 and 4T1 and MCF7 until passage 30.

2.10. Preliminary antitumour assay

A preliminary SRB assay using **1** and **1_AuNPs** (0.35 μM) on the aggressive MDA-MB-231 breast cancer cell line was carried out in PBS. Doxorubicin (**DOX**) was used as a positive control as the standard of care for many breast cancer subtypes in clinics, with an IC_{50} concentration of 0.091 μM. Growth obtained with control (PBS for **AuNPs**, DMSO for **1**, and **DOX** (0.091 μM)) was set as 100 %; data were presented as a mean ± SEM of 2 replicates (n = 2). Statistical significance was set to $p < 0.05$ for **1_AuNPs** (Ordinary one-way ANOVA, Dunnett's test).

2.11. Viability assay

HDF cells, 4T1 and MCF7 (1×10^4) were seeded in a 96-well plate and allowed to adhere for 24 h. Then, cells were treated with **DOX** (0.1 mM), **1** (0.1 mM), **1_AuNPs** (0.1 mM) and **AuNPs** (0.1 mM) at different concentrations for 24 h. Assessment of viability was performed using MTT colorimetric assay to quantify the cell metabolic activity. Briefly, cells were incubated with NPs for 24 h and after, media was removed and replaced with 0.5 mg/mL MTT in complete media and further incubated for 1 h. Media was removed, and formazan crystals were dissolved in 100 μL of DMSO (Supleco, pure grade). Absorbance was quantified at 570 nm using a plate reader (SpectraMax M5, Molecular devices). Results were expressed as percentage of viable cells relative to non-treated cells (100 % viability).

2.12. Statistics

All *in vitro* experiments were performed in triplicate (n = 3). Data in bar graphs were expressed as mean ± s.e.m. Statistical analysis was performed using GraphPad Prism by one-way ANOVA, followed by Bonferroni post hoc analysis when comparing three or more groups. No collected data were excluded from the analysis. The p-value is either reported in the manuscript text or shown in Figures and legends as

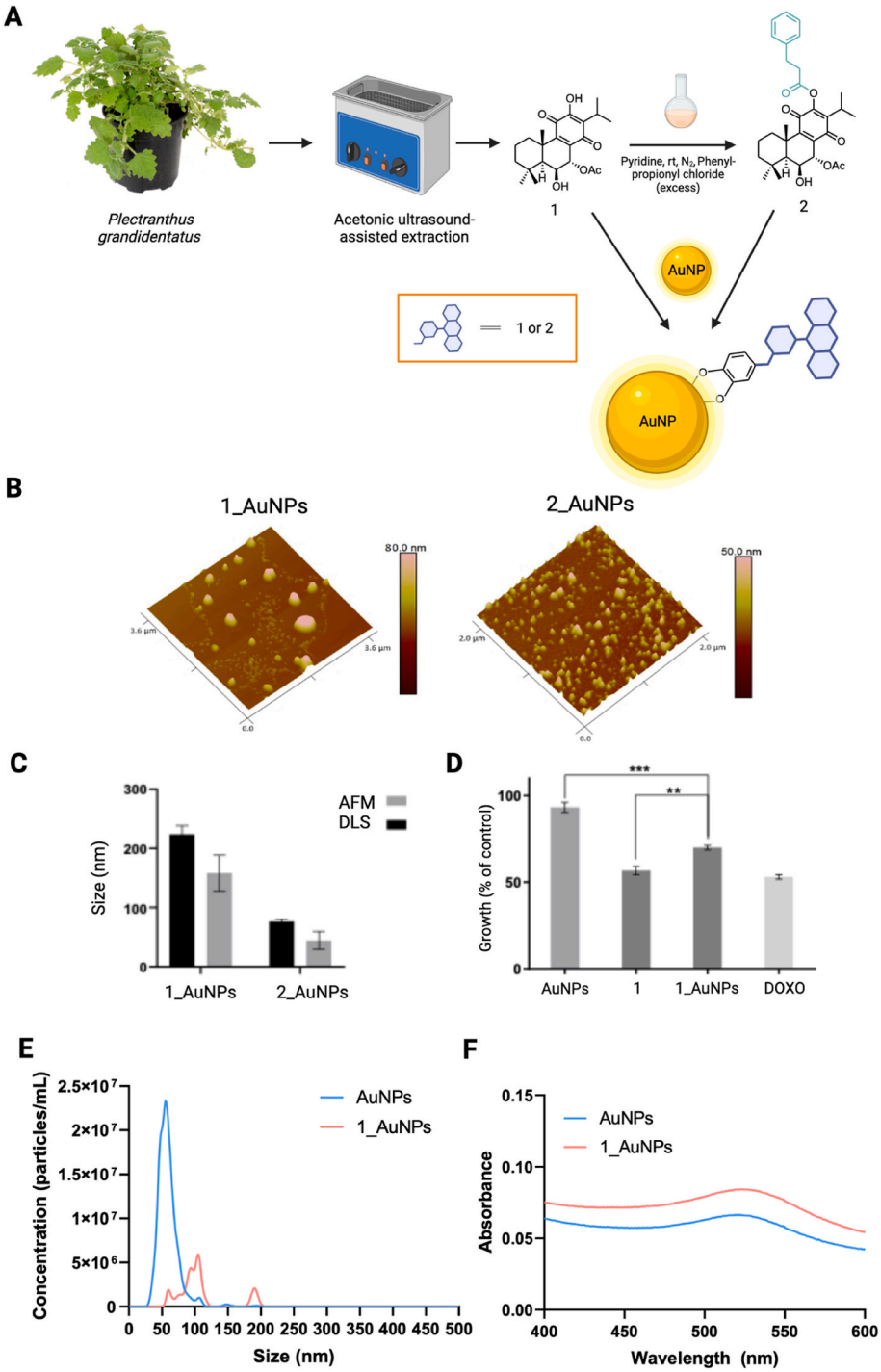

Fig. 1. Characteristics of functionalised royleanone AuNPs. **A)** Scheme of extraction of lead compound 7α-acetoxy-6β-hydroxyroyleanone (Roy, **1**), semi-synthesis of its ester derivative 7α-acetoxy-6β-hydroxy-12-*O*-(3-phenyl)propionylroyleanone (**2**) and consequent formation of AuNPs; **B)** AFM images of drug conjugated AuNPs: **1_AuNPs** and **2_AuNPs**; **C)** Comparative analysis of techniques used to measure **1_AuNPs** (0.1 mM) and **2_AuNPs** (0.02 mM) mean size determined by DLS (black columns) and AFM (grey columns). Data are represented as mean value ± SD, n = 3. Statistical significance: $p < 0.002$ compared to the average hydrodynamic diameter of the same type of particles determined by DLS and AFM; **D)** Antiproliferative effect on MDA-MB-231 breast cancer cell line of **1** and **1_AuNPs** (0.35 μM), assessed by sulforhodamine B (SRB) assay, after 48-h treatment. Growth obtained with control (PBS for **AuNPs**, DMSO for **1**, and **DOXO** (0.091 μM)) was set as 100 %; data are mean ± SEM of 2 replicates (n = 2); *$p < 0.05$, significantly different from **1_AuNPs** (Ordinary one-way ANOVA, Dunnett's test); **E)** Average size of drug conjugated **1_AuNPs** and unconjugated **AuNPs** using NTA; **F)** UV–VIS spectra of **AuNPs** and **1_AuNPs** showing slight shift in absorbance.

follows: *p < 0.05, **p < 0.01, ***p < 0.001, or ****p < 0.0001.

3. Results & discussion

3.1. Roy-functionalised AuNPs synthesis and physicochemical characterization

The AuNPs were synthesized using the Turkevich method, a process that uses a gold precursor (Gold(III) chloride trihydrate) and sodium citrate dihydrate [43]. The Turkevich method is a simple and widely used technique for synthesizing gold nanoparticles, by reducing chloroauric acid ($HAuCl_4$) with trisodium citrate in water. The citrate reduces gold ions (Au^{3+}) to atoms and stabilizes the resulting nanoparticles. Heating the mixture initiates nucleation and growth, producing mostly spherical particles around 10–30 nm in size. The method is popular due to its ease, low cost and biocompatibility.

Given the anti-cancer properties of abietane diterpenoids extracted from *Plectranthus* spp. previously described [20–23,31,35,39], we decided to investigate the potential cytotoxic effect of royleanones. Specifically, we focused on the lead compound Roy **(1)** and its derivative 7α-acetoxy-6β-hydroxy-12-*O*-(3-phenyl)propionylroyleanone **(2)** (Fig. 1A).

AuNPs functionalised with royleanones **1** or **2** were prepared according to Garcia et al. (2018) [22], by mixing a solution of AuNPs with acetonic solutions of **1** or **2**. In this preliminary study, three concentrations (0.02 mM, 0.1 mM, and 5 mM) were evaluated for each royleanone (**1** and **2**). The physicochemical properties of the different AuNPs functionalised with the royleanones at different concentrations and loading efficiencies are shown in Table 1. All tested concentrations (0.02 mM, 0.1 mM, and 5 mM) resulted in the successful synthesis of AuNPs functionalised to **1** (**1_AuNPs**). However, for the derivative **2** (**2_AuNPs**), at the 5 mM concentration, a yellow precipitate formed producing particles outside the nanoscale range and preventing the synthesis of **2_AuNPs** at this concentration (data not shown). While the 5 mM concentration was excessively high, causing precipitation for both **1** and **2**, the 0.02 mM concentration was notably low, with a negligible loading efficiency. In contrast, the 0.1 mM concentration achieved a drug loading efficiency of 74.9 %, providing stable **1_AuNPs** (Table 1). The reduced loading efficiency of **2_AuNPs** (6.3 %) is likely due to the ester group bound at the most reactive position 12-hydroxy (OH), leaving only the C6-OH position available for functionalization with gold, which complicates achieving the desired product. This is further highlighted by the substantial difference in yields at equimolar concentrations: 74.9 % for **1_AuNPs** versus just 6.3 % for **2_AuNPs**. Notably, the NPs obtained remained dispersed even at the higher concentration of 5 mM, representing a significant improvement over **1** alone.

Roylenanone abietanes isolated from the *Plectranthus* spp. have long been used in traditional medicine systems in southern Africa and their medicinal use continues to be scientifically validated. In fact, most recently, Dominguez et al. (2022) reported on the antiglioblastoma activity of the abietane diterpene parvifloron D, in which the authors recorded an activity of the diterpenoid far greater than that of the current clinical drug temozolomide (first-line treatment) [44]. Yet, these potential drugs present poor solubility in water. For this reason, the functionalization of AuNPs with the natural compound **1**, thanks to two OH groups at positions 6 and 12 on the second and third rings, respectively, may provide a solution to the low solubility issue by enhancing their therapeutic effect. As seen from the data on loading efficiency of **1** and **2**, the esterification of the OH group at position 12 seems to have impacted the ability of the compound to bind to the AuNPs, providing interesting information on structure-activity relationships and further confirming the importance of hydroxy loading sites for drug functionalization.

The **1_AuNPs** were successfully obtained with sizes between 29 and 54 nm and concentrations between 0.02 mM and 5 mM, respectively, as outlined in Table 1. This result is particularly promising given optimal size for cancer therapy applications places NPs diameter between the ranges of 10 and 100 nm [45]. At this size NPs can efficiently deliver drugs and achieve enhanced permeability and retention (EPR), which makes tumour's vasculature generally leaky.

Additionally, the AFM images of the **1_AuNPs** (0.1 mM), shown in Fig. 1B, revealed particles with spherical shapes. Although there was some variability in size, indicating different levels of AuNPs functionalization, the particles generally retained a spherical morphology. In contrast, the **2_AuNPs** (0.02 mM) depicted in Fig. 1B exhibited spherical-pyramidal shapes with more uniform sizes. The AFM images of **2_AuNPs** also showed a smaller hydrodynamic diameter, suggesting lower AuNPs functionalization, which correlates with the observed low loading efficiency. A comparison between DLS and AFM measurements is depicted in Fig. 1C. AFM measurements indicated smaller particle sizes for both **1_AuNPs** and **2_AuNPs** compared to those measured by DLS. This inconsistency contrasts with literature expectations, which suggest that AFM and DLS results should be closely aligned [46]. Indeed, the properties of the particles under analysis, such as their shape, composition, and aggregation state, can greatly affect the differences observed between measurement techniques. DLS is most effective for assessing particle sizes in monodisperse or nearly monodisperse samples. However, when particles are polydisperse, as indicated by the AFM images (Fig. 1C), DLS measurements may become less accurate and reliable [47]. Further data on the size and concentration of the **AuNPs** and the conjugated **1_AuNPs** was obtained using NTA, indicating one population for **AuNPs** at 58.5 ± 4 nm and two population sizes for **1_AuNPs** with an average size of 110.0 ± 11 nm, as shown in Fig. 1E. To confirm the successful conjugation of **1** to the NPs, UV–VIS showed a wavelength shift at which absorption was recorded (Fig. 1F).

Since the loading efficiency of **2_AuNPs** (6.3 %) was considerably low, functional studies were pursued only with **1_AuNPs** at the highest concentration, to obtain as much natural compound as possible attached into the NPs surface [42].

Table 1
Physicochemical characterization of hybrid royleanone AuNPs and their calculated loading efficiencies, deduced using Dynamic Light Scattering (DLS).

Nanoformulation/ concentration (mM)	Size (nm)	PDI	ZP	Loading efficiency (%)
AuNPs	26.22	0.351	−8.63	–
1_AuNPs/0.02	50.17	0.244	−8.02	–
1_AuNPs/0.1	29.37	0.399	−6.84	74.9 %
1_AuNPs/5	53.99	0.355	−8.71	22.6 %
2_AuNPs/0.02	76.26	0.293	−15.77	–
2_AuNPs/0.1	219.84	0.175	−3.97	6.3 %

PDI: Polydispersity index; ZP: Zeta Potential. Data are represented as mean value ± SD, n = 3. Statistical significance: p < 0.002 compared to the average hydrodynamic diameter of the same type of particles determined by DLS.

3.2. Antitumour evaluation

A preliminary sulforhodamine B (SRB) assay with a 48 h treatment period [48] was conducted with serial dilutions of **1** (ranging from 0.1 to 30.0 μM) to evaluate if **1_AuNPs** had antitumour properties. To study the cytotoxic activity of **1**, the aggressive MDA-MB-231 breast cancer cell line was tested. Eventually, **1** and **1_AuNPs** were tested at a concentration of 0.35 μM in PBS. **DOX** was used as a positive control, as it is the standard of care for many breast cancer subtypes in clinics, with an IC_{50} concentration of 0.091 μM. **AuNPs** did not significantly affect cell growth. In contrast, the drug delivery system **1_AuNPs** markedly reduced the growth rate of MDA-MB-231 cancer cells compared to **AuNPs** (Fig. 1D). These preliminary results demonstrated the sustained antitumour activity of the roylenanone abietanes when functionalised with AuNPs. In fact, the antitumour efficacy of **1_AuNPs** and **1** was very similar, however, since NPs can be directed into the tumour site

increasing the drug solubility and protecting the cargo from heading off target, the local concentration of the drug **1** in the AuNPs formulation will be higher, providing a more selective treatment. To better understand the cytotoxic effect of the natural compound, further studies using other cell lines for breast cancer were explored [36].

To determine the anti-cancer activity of the novel nanoformulation in comparison to **1** alone, an *in vitro* cancer cell model of breast cancer was used using murine 4T1 cells, human MCF7 cells and healthy human fibroblasts (HDF), as non-target control cells, to confirm the safety of the nanoformulation (Fig. 2). All cells were incubated for 24 h with the different samples, **DOX** alone, **1** alone, **AuNPs** and **1_AuNPs** at 10 serial concentrations. As expected, **DOX** caused cytotoxicity in all cell lines, even at lower concentrations with an IC_{50} for 4T1 cells of 1.43 μM, for MCF7 of 3.97 μM, and for HDF of 7.15 μM (Fig. 2A). Meanwhile,

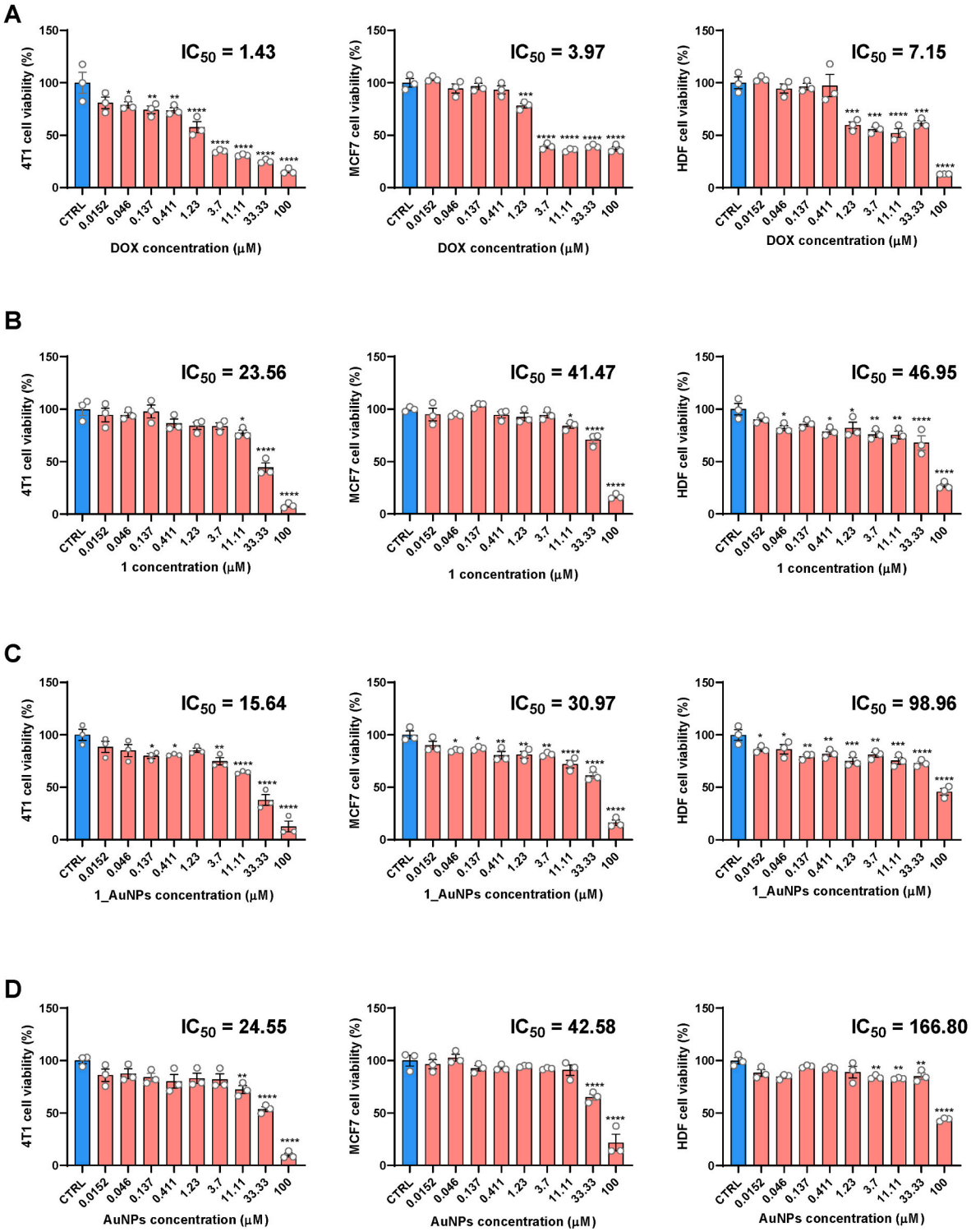

Fig. 2. *In vitro* cancer cell model of breast cancer 4T1 (mice), MCF7 (human) and HDF (healthy human) were treated for 24 h with **A)** doxorubicin (DOX), **B) 1**, **C) 1_AuNPs** and **D) AuNPs** to probe drug efficacy. Data are presented as mean ± s.e.m. P values were determined by one-way ANOVA with Bonferroni's correction treated vs. CTRL *$p < 0.05$, **$p < 0.01$, ***$p < 0.001$ and ****$p < 0.0001$.

1_AuNPs showed higher cytotoxicity than unfunctionalised **1** or free **AuNPs** in both breast cancer cell lines (IC_{50} for 4T1 cells of 15.64 μM and for MCF7 of 30.97 μM), showcasing the improved biological effect of the drug-functionalised nanoformulations when compared to the natural compound **1** alone. Furthermore, **1_AuNPs** showed better selectivity for cancer cells over HDF cells, as demonstrated by the higher HDF IC_{50} (98.96 μM) in comparison with 4T1 or MCF7 cells. In fact, the IC_{50} for **1** was 23.56 μM, and 24.55 μM for **AuNPs** in 4T1 cells. In addition, the difference between IC_{50} values of **DOX** among the three cell lines is much lower than the difference observed for the **1_AuNPs**. This observation suggests a marked improvement in the standard of care.

Drug-functionalised AuNPs have been exploited in the last years for their use as standard chemotherapy agents [49]. For example, methotrexate (MTX), was conjugated into a AuNPs system (MTX_AuNPs) and evaluated for its cytotoxic effects *in vitro* and antitumour activity *in vivo*. MTX bound directly to AuNPs through its carboxylic group (–COOH), forming the MTX_AuNPs complex, allowing for a controlled release of MTX over time. Importantly, MTX_AuNPs demonstrated greater cytotoxicity across various tumour cell lines in comparison with an equivalent dose of free MTX, likely due to the "concentrated effect" of the MTX_AuNPs complex [50]. In our case, the natural compound Roy (**1**), having also OH groups available for functionalization to AuNPs, demonstrated the same phenomena culminating in what we believe to be the first study of the royleanone compound **1** into improved cytotoxic gold nanoformulations for cancer therapy.

The increased therapeutic window of **1** through its functionalization to AuNPs, allows for higher doses to be administrated, thanks to their preferential effect in tumour cells than in healthy cells. It is worth mentioning that even though the results are promising, they are *in vitro*, and no targeting moiety is attached to the NPs. Nevertheless, it must be stated that most clinically approved antitumour nanoformulations are non-actively targeted to tumors and, nonetheless, they are approved. This could be attributed to the EPR effect that occurs in the tumour microenvironment. Thus, the same principle could benefit the efficacy of our strategy *in vivo*. Overall, it can be stated that the functionalization of the AuNPs with compound **1** to increase its solubility rate demonstrated its efficiency as a potential therapeutic drug to be used for breast cancer therapy.

4. Conclusions

Despite ample data on abietanes as cytotoxic agents, their high hydrophobicity results in poor aqueous solubility and decreased bioavailability, limiting their therapeutic application. This study showcases a preliminary investigation into royleanone nanoformulations, combining AuNPs with naturally occurring diterpenoids to increase the drug solubility and selective targeting towards the tumour microenvironment. Both diterpenoids functionalised with AuNPs were successfully synthesized, however, the royleanone diterpene presented more homogeneous AuNPs with a higher conjugation efficiency. This nanoformulation showcased improved functional activities when compared to the non-functionalised royleanone, demonstrating a high selectivity for cancer cells over healthy fibroblasts. These findings mark a significant step forward in developing new drug delivery platforms for cancer treatment.

CRediT authorship contribution statement

Gabrielle Bangay: Writing – review & editing, Writing – original draft, Software, Methodology, Investigation, Formal analysis, Data curation. **Vera M.S. Isca:** Writing – review & editing, Writing – original draft, Software, Methodology, Investigation, Formal analysis, Data curation. **João Morais:** Investigation. **Jennifer Fernández Alarcón:** Writing – review & editing, Writing – original draft, Methodology, Investigation. **Ana S. Viana:** Methodology. **Catarina P. Reis:** Methodology. **Catarina Pereira-Leite:** Writing – review & editing, Methodology. **Ana M. Díaz-Lanza:** Supervision. **Lucília Saraiva:** Methodology. **Cristina Fornaguera:** Writing – review & editing, Writing – original draft, Project administration. **Patricia Rijo:** Supervision, Resources, Project administration, Funding acquisition, Conceptualization.

Declaration of competing interest

The authors declare that they have no known competing financial interests or personal relationships that could have appeared to influence the work reported in this paper.

Acknowledgements

The authors acknowledge and thank Fundação para a Ciência e a Tecnologia (FCT, Portugal) for funding this project through DOI 10.54499/UIDP/04567/2020, DOI 10.54499/UIDB/04567/2020, UI/BD/151422/2021. This study was also supported by the following: AGAUR-Generalitat de Catalunya (2021 SGR 00537); ACCIO-Generalitat de Catalunya (grant agreement no. ACE05322000116); MICIN/AEI (PID2021-125910OB-I00, MCIN/AEI/10.13039/501100011033/FEDER, UE) and by Nuclis Program, from Generalitat de Catalunya (ACE053-GeneMarf).

Data availability

Data will be made available on request.

References

[1] S. Gulla, D. Lomada, V.V.S.S. Srikanth, et al., Chapter 11 - recent advances in nanoparticles-based strategies for cancer therapeutics and antibacterial applications, in: V. Gurtler, A.S. Ball, SBTM. in M. Soni (Eds.), Nanotechnology, vol. 46, Academic Press, 2019, pp. 255–293, https://doi.org/10.1016/bs.mim.2019.03.003.
[2] T. Sim, C. Lim, N.H. Hoang, et al., Nanomedicines for oral administration based on diverse nanoplatform, J. Pharm. Investig. 46 (2016) 351–362.
[3] A.R. Sharma, Y.H. Lee, A. Bat-Ulzii, M. Bhattacharya, C. Chakraborty, S.S. Lee, Recent advances of metal-based nanoparticles in nucleic acid delivery for therapeutic applications, J. Nanobiotechnol. 20 (1) (2022) 501, https://doi.org/10.1186/s12951-022-01650-z.
[4] R. Watkins, L. Wu, C. Zhang, R.M. Davis, B. Xu, Natural product-based nanomedicine: recent advances and issues, Int. J. Nanomed. 10 (2015) 6055–6074, https://doi.org/10.2147/IJN.S92162.
[5] J. Fernandez Alarcon, M. Soliman, T.U. Lüdtke, et al., Long-term retention of gold nanoparticles in the liver is not affected by their physicochemical characteristics, Nanoscale 15 (19) (2023), https://doi.org/10.1039/d3nr00685a.
[6] L. Talamini, P. Picchetti, L.M. Ferreira, et al., Organosilica cages target hepatic sinusoidal endothelial cells avoiding macrophage filtering, ACS Nano 15 (6) (2021), https://doi.org/10.1021/acsnano.1c00316.
[7] A. Ferreira, J. Alarcon, F. Guffanti, et al., Tuning of ultrasmall gold nanoparticles surface properties affect their biological fate, Part. Part. Syst. Char. 41 (2024), https://doi.org/10.1002/ppsc.202300168.
[8] G.A. Silva, Introduction to nanotechnology and its applications to medicine, Surg. Neurol. 61 (3) (2004) 216–220, https://doi.org/10.1016/j.surneu.2003.09.036.
[9] M.Z. El-Readi, M.A. Althubiti, Cancer nanomedicine: a new era of successful targeted therapy, J. Nanomater. 2019 (2019) 1–13.
[10] J. Liu, R. Zhang, Z.P. Xu, Nanoparticle-based nanomedicines to promote cancer immunotherapy: recent advances and future directions, Small 15 (32) (2019) 1900262.
[11] C.O. Silva, J.O. Pinho, J.M. Lopes, A.J. Almeida, M.M. Gaspar, C. Reis, Current trends in cancer nanotheranostics: metallic, polymeric, and lipid-based systems, Pharmaceutics 11 (1) (2019), https://doi.org/10.3390/pharmaceutics11010022.
[12] L.F.A. Al-Barram, S.M.H. Al-Jawad, A.A. Taha, N.J. Imran, Photothermal therapy of cancer cells enhanced by glutathione (GSH) modified small-sized gold nanoparticles, J. Electromagn. Waves Appl. 34 (18) (2020), https://doi.org/10.1080/09205071.2020.1822759.
[13] A.A. Taha, S.M.H. Al-Jawad, L.F.A. Al-Barram, Improvement of cancer therapy by TAT peptide conjugated gold nanoparticles, J. Cluster Sci. 30 (2) (2019), https://doi.org/10.1007/s10876-019-01497-9.
[14] M.Z. Ahmad, S. Akhter, G.K. Jain, et al., Metallic nanoparticles: technology overview & drug delivery applications in oncology, Expet Opin. Drug Deliv. 7 (8) (2010) 927–942.
[15] J. Lopes, T. Ferreira-Gonçalves, I.V. Figueiredo, et al., Proof-of-concept study of multifunctional hybrid nanoparticle system combined with nir laser irradiation for the treatment of melanoma, Biomolecules 11 (4) (2021), https://doi.org/10.3390/biom11040511.

[16] Moutaoukil M. El, M.G. Lolli, S. D'Amone, et al., Doxorubicin and NFL-TBS.40-63 peptide loaded gold nanoparticles as a multimodal therapy of glioblastoma, Discover Nano. 20 (1) (2025) 72, https://doi.org/10.1186/s11671-025-04249-z.

[17] Ali S. Shamim, T. Ali, H. Sharma, B.N. Kishor, S.K. Jha, Recent advances in monodisperse gold nanoparticle delivery, synthesis, and emerging applications in cancer therapy, Plasmonics (2025), https://doi.org/10.1007/s11468-024-02732-4. Published online.

[18] C. Garcia, V.M.S. Isca, F. Pereira, et al., Royleanone derivatives from Plectranthus spp. as a novel class of P-Glycoprotein inhibitors, Front. Pharmacol. 11 (2020), https://doi.org/10.3389/fphar.2020.557789.

[19] V.M.S. Isca, M. Sencanski, N. Filipovic, et al., Activity to breast cancer cell lines of different malignancy and predicted interaction with protein kinase C isoforms of royleanones, Int. J. Mol. Sci. 21 (10) (2020), https://doi.org/10.3390/ijms21103671.

[20] C. Garcia, C. Teodósio, C. Oliveira, et al., Naturally occurring plectranthus-derived diterpenes with antitumoral activities, Curr. Pharm. Des. 24 (36) (2019) 4207–4236, https://doi.org/10.2174/1381612825666190115144241.

[21] C. Garcia, E. Ntungwe, A. Rebelo, et al., Parvifloron D from plectranthus strigosus: cytotoxicity screening of Plectranthus spp. extracts, Biomolecules 9 (10) (2019), https://doi.org/10.3390/biom9100616.

[22] C. Garcia, C.O. Silva, C.M. Monteiro, et al., Anticancer properties of the abietane diterpene 6, 7-dehydroroyleanone obtained by optimized extraction, Future Med. Chem. 10 (10) (2018) 1177–1189, https://doi.org/10.4155/fmc-2017-0239.

[23] A. Santos-Rebelo, C. Garcia, C. Eleutério, et al., Development of parvifloron D-loaded smart nanoparticles to target pancreatic cancer, Pharmaceutics 10 (4) (2018), https://doi.org/10.3390/pharmaceutics10040216.

[24] O. Adedokun, E.N. Ntungwe, C. Viegas, et al., Enhanced anticancer activity of Hymenocardia acida stem Bark extract loaded into PLGA nanoparticles, Pharmaceuticals 15 (5) (2022), https://doi.org/10.3390/ph15050535.

[25] A. Hussain, M. Oves, M.F. Alajmi, et al., Biogenesis of ZnO nanoparticles using Pandanus odorifer leaf extract: anticancer and antimicrobial activities, RSC Adv. 9 (27) (2019) 15357–15369.

[26] H. Jahangirian, E.G. Lemraski, T.J. Webster, R. Rafiee-Moghaddam, Y. Abdollahi, A review of drug delivery systems based on nanotechnology and green chemistry: green nanomedicine, Int. J. Nanomed. 12 (2017) 2957.

[27] S. Bakrim, A. Balahbib, H.N. Mrabti, R. Ghchime, N. El Omari, A. Bouyahya, Chapter 16 - Nanophytomedicines: a Novel Approach for Improving Therapeutics via Delivery of Herbal Medicine, in: M.S. Hasnain, A.K. Nayak, T.M. Aminabhavi (Eds.), Advanced Nanoformulations: Theranostic Nanosystems vol. 3, Academic Press, 2023, pp. 431–465, https://doi.org/10.1016/B978-0-323-85785-7.00011-5.

[28] M. Elmowafy, K. Shalaby, M.H. Elkomy, et al., Polymeric nanoparticles for delivery of natural bioactive agents: recent advances and challenges, Polymers (Basel) 15 (5) (2023), https://doi.org/10.3390/polym15051123.

[29] S. Peng, Y. Wang, Z. Sun, et al., Nanoparticles loaded with pharmacologically active plant-derived natural products: biomedical applications and toxicity, Colloids Surf. B Biointerfaces 225 (2023) 113214, https://doi.org/10.1016/j.colsurfb.2023.113214.

[30] C.O. Silva, S.B. Petersen, C.P. Reis, et al., EGF functionalized polymer-coated gold nanoparticles promote EGF photostability and EGFR internalization for photothermal therapy, PLoS One 11 (10) (2016), https://doi.org/10.1371/journal.pone.0165419.

[31] E. Ntungwe, E.M. Domínguez-Martín, G. Bangay, et al., Self-assembly nanoparticles of natural bioactive abietane diterpenes, Int. J. Mol. Sci. 22 (19) (2021), https://doi.org/10.3390/ijms221910210.

[32] C.A.G. Garcia, Isolation, Synthesis and Nanoencapsulation of Cytotoxic Compounds from Plectranthus Spp, Universidad de Alcalá, 2019.

[33] C. García, C.E.S. Bernardes, M.F.M. Piedade, et al., Dehydroroyleanone as a building block for a drug delivery platform based on self-assembled nanoparticles: structural studies and chemical modification, ACS Omega 7 (48) (2022) 44180–44186, https://doi.org/10.1021/acsomega.2c05353.

[34] C.O. Silva, J. Molpeceres, B. Batanero, et al., Functionalized diterpene parvifloron D-loaded hybrid nanoparticles for targeted delivery in melanoma therapy, Ther. Deliv. 7 (8) (2016) 521–544, https://doi.org/10.4155/tde-2016-0027.

[35] A. Santos-Rebelo, P. Kumar, V. Pillay, et al., Development and mechanistic insight into the enhanced cytotoxic potential of parvifloron D albumin nanoparticles in EGFR-overexpressing pancreatic cancer cells, Cancers (Basel) 11 (11) (2019), https://doi.org/10.3390/cancers11111733.

[36] A.A.M. Saeed, E.M.A. Mohsen, A.R.A. Bin Yahia, Eco-friendly synthesis, characterization, and anticancer potential of iron oxide nanoparticles derived from Plectranthus amboinicus and Dorstenia foetida plant extracts, Green Chem. Lett. Rev. 18 (1) (2025) 2525090, https://doi.org/10.1080/17518253.2025.2525090.

[37] K.X. Lee, K. Shameli, Y. Nagao, Y.P. Yew, S.Y. Teow, H. Moeini, Potential use of gold-silver core-shell nanoparticles derived from Garcinia mangostana peel for anticancer compound, protocatechuic acid delivery, Front. Mol. Biosci. 9 (2022), https://doi.org/10.3389/fmolb.2022.997471.

[38] I. Neto, E.M. Domínguez-Martín, E. Ntungwe, et al., Dehydroabietic acid microencapsulation potential as biofilm-mediated infections treatment, Pharmaceutics 13 (6) (2021), https://doi.org/10.3390/pharmaceutics13060825.

[39] C.E.S. Bernardes, C. Garcia, F. Pereira, et al., Extraction optimization and structural and thermal characterization of the antimicrobial Abietane 7α-Acetoxy-6β-hydroxyroyleanone, Mol. Pharm. 15 (4) (2018) 1412–1419, https://doi.org/10.1021/acs.molpharmaceut.7b00892.

[40] M. Hensch, P. Rüedi, C.H. Eugster, Horminon, Taxochinon und weitere Royleanone aus 2 abessinischen Plectranthus-Spezies (Labiatae), Helv. Chim. Acta 58 (7) (1975), https://doi.org/10.1002/hlca.19750580707.

[41] V.M.S. Isca, G. Bangay, S. Princiotto, et al., Extraction optimization and reactivity of 7α-acetoxy-6β-hydroxyroyleanone and ability of its derivatives to modulate PKC isoforms, Sci. Rep. 14 (1) (2024) 16990, https://doi.org/10.1038/s41598-024-67384-0.

[42] Isca VMS, dos Santos DJVA, Matos AC, et al. Protein Kinase-α Modulation for Breast Cancer Therapy with 7α-acetoxy-6β-hydroxyroyleanone Derivatives Based on Molecular Docking Studies. *(under submission)*.

[43] J. Turkevich, P. Stevenson, Faraday JHD of the, 1951 undefined. A study of the nucleation and growth processes in the synthesis of colloidal gold, pubs.rsc.orgJ Turkevich, PC Stevenson, J Hillier, Discuss. Faraday Soc. 47 (2) (1941), 1951•pubs.rsc.org..

[44] M. Magalhães, E.M. Domínguez-Martín, J. Jorge, et al., Parvifloron D-based potential therapy for glioblastoma: inducing apoptosis via the mitochondria dependent pathway, Front. Pharmacol. 13 (2022), https://doi.org/10.3389/fphar.2022.1006832.

[45] Y. Yao, Y. Zhou, L. Liu, et al., Nanoparticle-based drug delivery in cancer therapy and its role in overcoming drug resistance, Front. Mol. Biosci. 7 (2020), https://doi.org/10.3389/fmolb.2020.00193.

[46] A. Santos-Rebelo, P. Kumar, V. Pillay, et al., Development and mechanistic Insight into the enhanced cytotoxic potential of parvifloron D albumin nanoparticles in EGFR-overexpressing pancreatic cancer cells, Cancers (Basel) 11 (11) (2019), https://doi.org/10.3390/cancers11111733.

[47] C.M. Maguire, M. Rösslein, P. Wick, A. Prina-Mello, Characterisation of particles in solution – a perspective on light scattering and comparative technologies, Sci. Technol. Adv. Mater. 19 (1) (2018) 732–745, https://doi.org/10.1080/14686996.2018.1517587.

[48] C. Bessa, J. Soares, L. Raimundo, et al., Discovery of a small-molecule protein kinase Cδ-selective activator with promising application in colon cancer therapy article, Cell Death Dis. 9 (2) (2018), https://doi.org/10.1038/s41419-017-0154-9.

[49] S. Jain, D.G. Hirst, J.M. O'Sullivan, Gold nanoparticles as novel agents for cancer therapy, Br. J. Radiol. 85 (1010) (2012), https://doi.org/10.1259/bjr/59448833.

[50] Y.H. Chen, C.Y. Tsai, P.Y. Huang, et al., Methotrexate conjugated to gold nanoparticles inhibits tumor growth in a syngeneic lung tumor model, Mol. Pharm. 4 (5) (2007), https://doi.org/10.1021/mp060132k.